Journal of the Korean Ceramic Society
Vol. 43, No. 11, pp. 724~727, 2006.

Experimental Verification of a Kinetic Model of Zr-Oxidation

Han-Ill Yoo† and Sang-Hyun Park

Solid State Ionics Research Lab., School of Materials Science and Engineering, Seoul National University, Seoul 151-744, Korea
(Received October 19, 2006; Accepted October 30, 2006)

ABSTRACT

It has long been known that the oxidation kinetics of Zr-based alloys undergoes a crossover from parabolic to cubic in the pre-transition period (before breakaway of the oxide scale). This kinetic crossover, however, is not fully understood yet. We have earlier proposed a model for the Zr-oxidation kinetics, in a closed form for the first time, by taking into account a compressive strain energy gradient as a diffusional driving force in addition to a chemical potential gradient of component oxygen across the ZrO_2 scale upon Zr [*J. Nucl. Mater.*, 299 (2001) 235]. In this paper, we experimentally reconfirm the validity of the proposed model by using the thermogravimetric data on mass gain of Zr in a plate and wire form, respectively, in air atmosphere at different temperatures in the range of 500° to 800°C, and subsequently report on the numerical values for oxygen chemical diffusivity and strain energy gradient across the oxide scale.

***Key words*: Oxidation kinetics, Zr-based alloys, ZrO_2, Oxygen chemical diffusivity, Strain energy**

1. Introduction

Oxidation kinetics of Zr is extremely important to predict the life time of various Zr-based structural components, e.g., pressure tubes and claddings, particularly in nuclear power plants. It has been repeatedly observed[1-4] that the oxidation kinetics of Zr-based alloys is very initially linear ($\Delta m \sim t$), followed seldom, or briefly if any, by a parabolic kinetics ($\Delta m \sim t^{1/2}$), but eventually turns to a cubic kinetics ($\Delta m \sim t^{1/3}$) until a final transition back to a linear kinetics ($\Delta m \sim t$) or breakaway of the oxide. Despite many attempts thus far, however, quantitative understanding of the kinetic shift from parabolic to cubic is still far from complete.[1,2]

Yoo *et al.*[1] (henceforth referred to as Ref. 1) have earlier proposed a kinetic model in a closed form to explain the sub-parabolic kinetics by taking into account the compressive strain energy gradient as a diffusional driving force in addition to the omnipresent oxygen potential gradient. The origin of the compressive stress is not yet elucidated unequivocally, but it is highly likely attributed to the metal/oxide lattice mismatch and/or chemical strain due to oxygen nonstoichiometry across the oxide scale.[1,2] In their treatment,[1] the authors assumed that this strain energy gradient is constant for the sake of mathematical simplicity and hence, they could establish a rate equation in a closed form. It was subsequently found that the rate equation surprisingly precisely describes the oxidation kinetics of Zr as observed via thermogravimetry in the temperature range of 400° to 800°C by the authors themselves. Consequently, they could evaluate the mean chemical diffusion coefficient of component oxygen as a function of temperature. Furthermore, assuming the critical thickness ξ_C of the oxide scale, where its breakaway is about to start, to be the thickness where the compressive stress completely relieves, they could even evaluate the compressive stress at the metal/oxide interface. Nevertheless, the model was tested only for one specific case and hence, its general validity or reproducibility has remained untested.

This paper aims to test and reconfirm the validity of the proposed model with the kinetic data obtained from Zr samples of different sources and different shapes from the earlier study in Ref. 1. We will start by briefly summarizing the kinetic model.

2. Kinetic Model

It is well known[5-9] that the oxide scale until its breakaway consists of tetragonal t-ZrO_2 and monoclinic m-ZrO_2 but with gradually decreasing fraction of the former from the Zr/ZrO_2 interface even at temperatures where m-ZrO_2 would otherwise be thermodynamically stable. This fact already indicates that there must be a compressive stress to stabilize t-ZrO_2, and the existence of a stress gradient has been confirmed experimentally.[2,10]

The strain energy per mole-O in the oxide may be written as[11,12]

$$u = \frac{V_m}{2}\frac{Y}{1-\nu}\varepsilon(x)^2 \quad (1)$$

where V_m, Y, and ν denote the molar volume, Young's modulus, and Poisson's ratio of ZrO_2, respectively, and $\varepsilon(x)$ strain

†Corresponding author : Han-Ill Yoo
E-mail : hiyoo@snu.ac.kr
Tel : +82-2-880-7163 Fax : +82-2-884-1413

at position x in the reaction product ZrO_2.

By taking into account the strain energy gradient ∇u as a diffusional driving force in addition to the omnipresent oxygen potential gradient $\nabla\mu_o$ across the oxide scale, one may obtain a kinetic equation for a planar geometry as

$$\frac{d\xi}{dt}=\frac{K_p}{\xi}-\beta \tag{2a}$$

or

$$t=-\frac{\xi}{\beta}-\frac{K_p}{\beta^2}\ln\left(1-\frac{\beta\xi}{K_p}\right) \tag{2b}$$

with

$$K_p=\frac{\overline{D}_o}{2RT}(-\Delta G);\quad \beta=\frac{\overline{D}_o}{RT}(-\nabla u) \tag{3}$$

where ξ is the thickness of the oxide scale as measured from the Zr/ZrO_2 interface (x=0), t the length of oxidation duration, $\overline{D}_o$ the spatial average of the oxygen diffusivity across ξ, ΔG the reaction free energy of the reaction $Zr+O_2=ZrO_2$, and the rest have their usual significance. It is reminded that in order to reach the integral form, Eq. (2b), the strain energy gradient ∇u was assumed to be constant. It is noted that Eq. (2) reduces to the conventional parabolic rate law $\xi^2=2K_pt$ as $\nabla u\rightarrow 0$. For detailed derivation, the reader is referred to Ref. 1.

3. Experimental

In the earlier work, Ref. 1, the specimens were Zr-plates of 99.9% purity, produced by CEZUS, France. In the present work, we chose Zr in a plate form with 1 mm thickness as well as in a wire form with 1 mm diameter, both with 99.2% purity from Alfa Aesar, USA. Each type specimen was oxidized in dry air atmosphere in a thermo-balance (Setaram TG/DTA 92-18, France) at different temperatures in the range of 500° to 800°C while monitoring mass increase Δm with time t with a resolution of ±1 μg. For experimental details, the reader is referred to Ref. 1.

4. Results and Discussions

The results from the plate specimens are as illustrated in Fig. 1, where the mass gain vs. time was translated into the oxide thickness ξ vs. t, assuming that in-diffusing oxygen atoms are all consumed for the oxidation of underlying Zr or in other words, neglecting the dissolution of oxygen into the base metal. (The correction against latter may be rather trivial at the steady state). As is seen, the oxide scales eventually exhibit a breakaway by turning back to the linear kinetics. (For the 500°C data shown, the breakaway is not shown in the figure because it occurs far outside the time scale shown in the figure). The kinetic behavior appears to be in excellent agreement with what was observed earlier in Ref. 1.

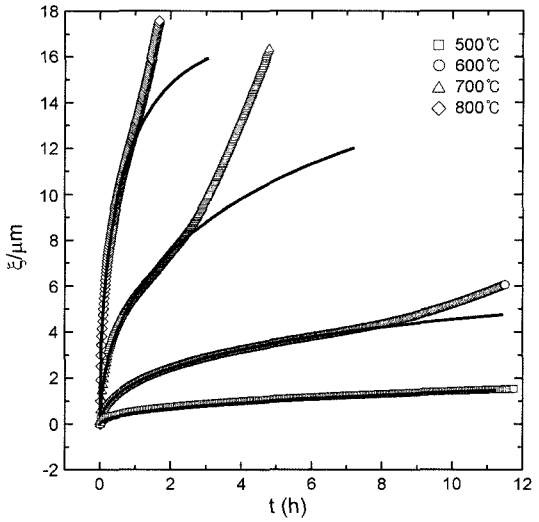

Fig. 1. Oxide scale thickness vs. time of Zr-plate specimens at different temperatures. The solid lines are the best-fitted to Eq. (2b) in the text.

The experimental data of ξ vs. t has been non-linear-least-squares fitted to Eq. (2b). As depicted by the solid lines in Fig. 1, Eq. (2b) describes precisely enough the kinetics until breakaway at all temperatures with the fitting parameters K_p and β evaluated as listed in the 2nd and 3rd row, respectively, in Table 1. It is emphasized that the fitting errors are no greater than 2% for K_p and 6% for β even in the worst case (700°C).

By using the numerical values for the reaction free energy ΔG[13] (4th row of Table 1), one can evaluate, via Eq. (3), the

Table 1. All the Numerical Values as Evaluated from the Oxidation Kinetics of Zr-Plates

Temperature (°C)	500	600	700	800
K_p/m^2s^{-1}	$(3.485\pm0.007)\times10^{-17}$	$(5.368\pm0.008)\times10^{-16}$	$(5.48\pm0.09)\times10^{-15}$	$(4.65\pm0.03)\times10^{-14}$
β/ms^{-1}	$(7.56\pm0.05)\times10^{-12}$	$(7.59\pm0.03)\times10^{-11}$	$(3.07\pm0.18)\times10^{-10}$	$(2.71\pm0.04)\times10^{-9}$
$\nabla\mu_{O_2}/J$	-9.40×10^5	-9.20×10^5	-9.00×10^5	-8.81×10^5
$\overline{D}_o/m^2s^{-1}$	$(4.77\pm0.01)\times10^{-19}$	$(8.470\pm0.013)\times10^{-18}$	$(9.85\pm0.16)\times10^{-16}$	$(9.42\pm0.06)\times10^{-16}$
$\nabla u/Jm^{-1}mol{\cdot}O^{-1}$	$(1.020\pm0.007)\times10^{11}$	$(6.50\pm0.03)\times10^{10}$	$(2.52\pm0.15)\times10^{10}$	$(2.57\pm0.04)\times10^{10}$
ξ_C/m	2.48×10^{-6}	4.12×10^{-6}	7.79×10^{-6}	1.20×10^{-5}
$u(0)/Jmol{\cdot}O^{-1}$	$(2.530\pm0.017)\times10^5$	$(2.682\pm0.011)\times10^5$	$(1.96\pm0.12)\times10^5$	$(3.08\pm0.05)\times10^5$

mean oxygen diffusivity $\overline{D}_o$.

The strain energy gradient, that has been assumed to be constant, is also evaluated from the values for β due to Eq. (3). The critical thickness ξ_C, corresponding to the position where $\varepsilon=0$, may also be assumed to be the thickness just before the breakaway, and hence, estimated to be the position where the extensions of the fitted Eq. (2) and final linear kinetics (after breakaway) in Fig. 1 meet each other. Subsequently, the strain energy at the Zr/ZrO_2 interface u(0) is evaluated as $u(0)=\nabla u\cdot\xi_C$. All the numerical values thus evaluated are summarized in Table 1.

On the other hand, the oxidation kinetics, ξ vs. t of the wire specimens are as shown in Fig. 2. As the critical thickness of oxide scale ξ_C (or the thickness up to the beginning of breakaway) is of the order of 20 μm at the highest temperature of examination, but normally much less, one may approximate the cylindrical geometry to be the planar geometry with the maximum relative error of $\xi_C/d=0.02$ (d=1 mm, the initial diameter of the wire specimen) in the worst case of 800°C. We have, thus, non-linear-least-squares-fitted the kinetic data in Fig. 2 to Eq. (2b). The results are depicted by solid lines in Fig. 2. As is clearly seen, Eq. (2) again elegantly describes all the kinetics.

The fitting parameters K_p and β in Eq. (2b) have been evaluated as listed in Table 2. As expected, the results at 800°C are subjected to the highest uncertainty, but the error bounds are still tolerable (2% and 5%, respectively). Following the same procedures as in the Zr-plate case (Table 1), $\overline{D}_o$, ∇u, and u(0) are subsequently evaluated and listed in Table 2.

In the present work, the parabolic rate law constant K_p has turned out to take a value in the range of 10^{-17} to 10^{-14} m^2/s and β in the range of 10^{-11} to 10^{-9} m/s depending on temperature for both plate and wire specimens. These values are quite close to those in Ref. 1 as expected.

The mean diffusivities of component oxygen are plotted against reciprocal temperature in Fig. 3 and best estimated as,

$$\overline{D}_o/m^2s^{-1}=(2.3^{+2.3}_{-1.2})\times10^{-7}\exp\left(-\frac{1.80\pm0.05\ eV}{kT}\right) \quad (4)$$

for the plate specimens, and

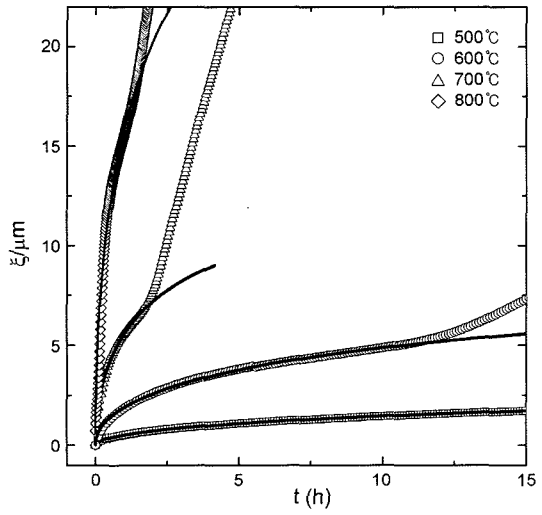

Fig. 2. Oxide scale thickness vs. time of Zr-wire specimens at different temperatures. The solid lines are the best-fitted to Eq. (2b) in the text.

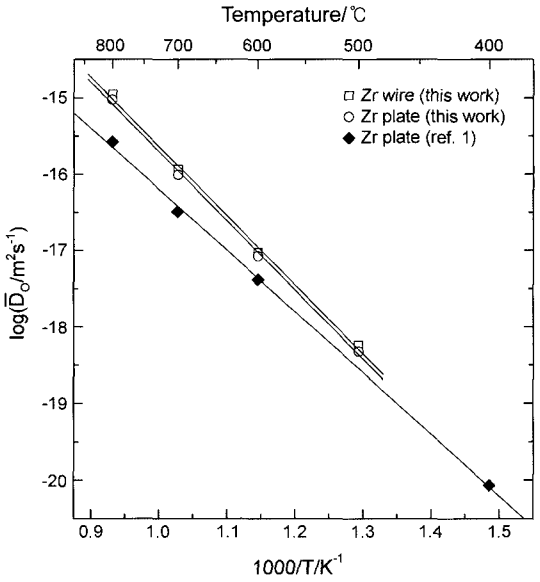

Fig. 3. Mean oxygen diffusivity vs. reciprocal temperature as obtained from Zr in plate forms and in wire forms, respectively.

Table 2. All the Numerical Values as Evaluated from the Oxidation Kinetics of Zr-Wires

Temperature (°C)	500	600	700	800
K_p/m^2s^{-1}	$(4.184\pm0.002)\times10^{-17}$	$(5.971\pm0.019)\times10^{-16}$	$(6.53\pm0.06)\times10^{-15}$	$(5.48\pm0.11)\times10^{-14}$
β/ms^{-1}	$(1.1801\pm0.0017)\times10^{-11}$	$(7.57\pm0.05)\times10^{-11}$	$(5.66\pm0.12)\times10^{-10}$	$(1.79\pm0.09)\times10^{-9}$
$\nabla\mu_{O_2}/J$	-9.40×10^5	-9.20×10^5	-9.00×10^5	-8.81×10^5
$\overline{D}_o/m^2s^{-1}$	$(5.721\pm0.003)\times10^{-19}$	$(9.42\pm0.03)\times10^{-18}$	$(1.174\pm0.011)\times10^{-16}$	$(1.11\pm0.02)\times10^{-15}$
$\nabla u/Jm^{-1}mol\cdot O^{-1}$	$(1.326\pm0.002)\times10^{11}$	$(5.83\pm0.04)\times10^{10}$	$(3.90\pm0.09)\times10^{10}$	$(1.44\pm0.08)\times10^{10}$
ξ_C/m	-	5.12×10^{-6}	6.93×10^{-6}	1.86×10^{-5}
$u(0)/Jmol\cdot O^{-1}$	-	$(2.99\pm0.02)\times10^5$	$(2.70\pm0.06)\times10^5$	$(2.68\pm0.14)\times10^5$

$$\overline{D}_o/m^2s^{-1} = (2.7^{+3.3}_{-1.5}) \times 10^{-7} \exp\left(-\frac{1.80 \pm 0.06\ eV}{kT}\right) \quad (5)$$

for the wire specimens. They are in excellent agreement with each other.

In the earlier work (Ref. 1) with a Zr-plate of different origin, the same diffusivity was estimated as

$$\overline{D}_o/m^2s^{-1} = (6.6^{+4.3}_{-2.6}) \times 10^{-9} \exp\left(-\frac{1.59 \pm 0.04\ eV}{kT}\right). \quad (6)$$

This is somewhat smaller than the present values, Eqs. (4) and (5), as compared in Fig. 3, probably reflecting a different quality of the Zr specimens in terms of impurity types and contents.

It was earlier found, from the open circuit voltage as measured across the growing oxide scale in Ref. 1, that the growing oxide is a mixed ionic-electronic conductor with a mean electronic transference number of ca. 0.5. This fact indicates that the diffusion coefficient of component oxygen must be of the Nernst-Planck type or

$$\overline{D}_o = \frac{RTV_m}{8F^2} \cdot \frac{\sigma_i \sigma_e}{\sigma_i + \sigma_e} \quad (7)$$

where σ_i and σ_e stand for the ionic conductivity by O^{2-} ions and electronic conductivity, respectively, of the oxide scale that is polycrystalline with gradually decreasing fraction of t-ZrO_2 with increasing thickness.

The strain energy at the Zr/ZrO_2 interface u(0) in the present case has been found to be of the order of magnitude of 10^5 J/mol-O, that is the same as in Ref. 1. When taking the Young's modulus of the oxide as that of sintered yttria-stabilized zirconia[14] or Y=200 GPa, and ν=0.3, and assuming the oxide breakaway to start as soon as the compressive strain fully relaxes to nill at $\xi=\xi_C$, the present strain energy values again lead, due to Eq. (1), to a compressive stress of the order of magnitude of 60 GPa as in Ref. 1. According to a recent measurement,[10] the compressive stress at the Zr/ZrO_2 interface increases with increasing thickness of the oxide scale and takes a value of 1~1.5 GPa when ξ=~2 μm. In this light, the stress evaluated in the present work is obviously too much overestimated and it may be attributed to the overestimation of the critical thickness of the oxide scale ξ_C. For the origins of the stress and more discussions, the reader is referred to Ref. 1.

5. Conclusion

We, thus, conclude that the validity of the proposed kinetic model of Zr-oxidation, Eq. (2) is reconfirmed. It is further supported that the sub-parabolic or cubic kinetics is attributed to the compressive strain energy gradient that counteracts the oxygen potential gradient as the driving forces for oxygen chemical diffusion. The mean chemical diffusion coefficient of oxygen across the oxide scale is on the order of magnitude of 10^{-19} to 10^{-15} m^2/s depending on temperature with an activation energy of 1.6–1.8 eV in the range of 500° to 800°C. The strain energy gradient, which is assumed to be constant in the present model, takes a value in the range of 10^{11} to 10^{10} J/m/mol-O, decreasing with increasing temperature.

REFERENCES

1. H.-I. Yoo, B.-J. Koo, J.-O. Hong, I.-S. Hwang, and Y.-H. Jeong, "A Working Hypothesis on Oxidation Kinetics of Zircaloy," *J. Nucl. Mater.*, **299** 235-41 (2001).
2. J. Favergeon, T. Montesin, and G. Bertrand, "Mechano-Chemical Aspects of High Temperature Oxidation: A Mesoscopic Model Applied to Zirconium Alloys," *Oxid. Met.*, **64** 253-79 (2005).
3. T. Ahmed and L. H. Keys, "The Breakaway Oxidation of Zirconium and Its Alloys. A Review," *J. Less-Common Met.*, **39** 99-107 (1975).
4. E. Hillner, "Corrosion of Zirconium-Base Alloys-An Overview"; vol. 633, pp. 211-35 in: Zirconium in the Nuclear Industry: Third International Symposium, ASTM STP, 1977.
5. M. Martin, N. Lakshmi, U. Koops, and H.-I. Yoo, "In Situ Investigations on the Oxidation of Metals," Proc. 16th Ikedani Conference, Electrochemistry and Thermodynamics on Materials Processing for Sustainable Production: Masuko Symposium, Nov. 12-16, 2006, Tokyo, Japan.
6. H.-J. Beie, A. Mitwalsky, F. Garzarolli, H. Ruhmann, and H.-J. Sell, "Examinations of the Corrosion Mechanism of Zirconium Alloys"; pp. 615-43 in: Zirconium in the Nuclear Industry: Tenth International Symposium, ASTM STP 1245, 1994.
7. F. Garzarolli, H. Seidel, R. Tricot, and J. P. Gros, "Oxide Growth Mechanism on Zirconium Alloys"; pp. 395-415 in: Zirconium in the Nuclear Industry: Ninth International Symposium, ASTM STP 1132, 1991.
8. J. Godlewski, "How the Tetragonal Zirconia is Stabilized in the Oxide Scale that is Formed on a Zirconium Alloy Corroded at 400°C in Steam"; pp. 663-83 in: Zirconium in the Nuclear Industry: Tenth International Symposium, ASTM STP 1245, 1994.
9. J. Godlewski, J. P. Gros, M. Lambertin, J. F. Wadier, and H. Weidinger, "Raman Spectroscopy Study of the Tetragonal-to-Monoclinic Transition in Zirconium Oxide Scales and Determination of Overall Oxygen Diffusion by Nuclear Microanalysis of O^{18}"; pp. 416-36 in: Zirconium in the Nuclear Industry: Ninth International Symposium, ASTM STP 1132, 1991.
10. J. Godlewski, P. Bouvier, G. Lucazeau, and L. Fayette, "Stress Distribution Measured by Raman Spectroscopy in Zirconia Films Formed by Oxidation of Zr-Based Alloys"; p. 877-900 in: Zirconium in the Nuclear Industry, Twelfth International Symposium (ASTM special technical publication), 2000.
11. H. Schmalzried, "Chemical Kinetics of Solids", pp. 331-54, VCH, Weinheim, Chap. 14, 1995.
12. S. P. Timoshenko and J. N. Goodier, Theory of Elasticity, 3rd Ed.; p. 247, McGraw-Hill, Inc., 1970.
13. L. B. Pankratz, Thermodynamic Properties of Elements and Oxides, PB83-174052, US Bureau of Mines, Albany, OR, 1983.
14. M. Barsoum, Fundamentals of Ceramics; p. 401, McGraw-Hill. Inc., 1997.